Cofilin Promotes Actin Polymerization and Defines the Direction of Cell Motility

Mousumi Ghosh,[1] Xiaoyan Song,[1] Ghassan Mouneimne,[1] Mazen Sidani,[1] David S. Lawrence,[2] John S. Condeelis[1]*

A general caging method for proteins that are regulated by phosphorylation was used to study the in vivo biochemical action of cofilin and the subsequent cellular response. By acute and local activation of a chemically engineered, light-sensitive phosphocofilin mimic, we demonstrate that cofilin polymerizes actin, generates protrusions, and determines the direction of cell migration. We propose a role for cofilin that is distinct from its role as an actin-depolymerizing factor.

Standard genetic, biochemical, and chemical tools have been unable to define the precise temporal and spatial contributions of the individual protein components of signaling pathways. For example, the precise intracellular role of cofilin during cellular migration has been difficult to decipher, because motility depends on localized transients of spatially well-defined signaling activity. Results obtained from cofilin overexpression are complicated by issues of compensation by phosphorylation (*1*, *2*), modulation of expression of other motility-related proteins (*3*), inappropriate localization of overexpressed protein (*4*–*7*), and lethality of cofilin suppression (*8*–*10*). Localized photoactivation of protein activity allows one to circumvent these problems (*11*). In order to establish the in vivo role of cofilin and its mechanistic contributions to cell motility, we prepared a mimic of inactive phosphocofilin that can be rapidly "switched on" by a brief burst of light. This modified protein is resistant to down-regulation by endogenous biochemical mechanisms. We examined the effects of both global and local release of cofilin activity on actin polymerization, depolymerization, protrusion, and motility. The instantaneous cell-wide photoactivation of cofilin activity increased free barbed ends, F-actin content, and cellular locomotion. Furthermore, highly localized intracellular cofilin activation generated lamellipodia and determined the direction of cell motility. Thus, cofilin, by defining the site of actin polymerization to form a protrusion, acts as a component of the "steering wheel" of the cell.

Activation of cofilin is required for cell motility (*12*–*14*). However, it is not clear how the activities of cofilin, which include barbed end formation and actin polymerization (*14*) as well as depolymerization (*12*), are coordinated. Nor has it been determined which of these activities predominate during protrusion and cell motility. Another unresolved question is the role of cofilin in chemotaxis. Recent analysis of the distribution of cofilin and phosphocofilin in migrating fibroblasts suggests a role for active cofilin at the leading edge (*15*). However, it remains unclear if cofilin actively sets the direction of cell motility, alters cell polarity, or serves a more indirect role, such as actin filament turnover. For example, it is possible that cofilin-induced polymerization could generate an initial asymmetric compartment that defines the high-affinity receptors for chemoattractants (*16*) as a site for subsequent recruitment and activation of phosphatidylinositol 3-kinase and Rho family G proteins. This would set the direction of cell movement and, therefore, chemotaxis. Further, it has been demonstrated in vitro that severing of existing actin filaments by cofilin initiates the side binding activity of Arp2/3 (*17*). Inside cells, this could lead to actin polymerization at the leading edge. The localized light-driven activation of cofilin activity is a means to address these issues.

We designed a caged (inactive) form of a constitutively active mutant of cofilin (S3C), which can be microinjected into cells and locally activated. The serine at position 3 was mutated to cysteine, and this S3C mutant cofilin was covalently modified with α-bromo-(2-nitrophenyl) acetic acid (BNPA) as

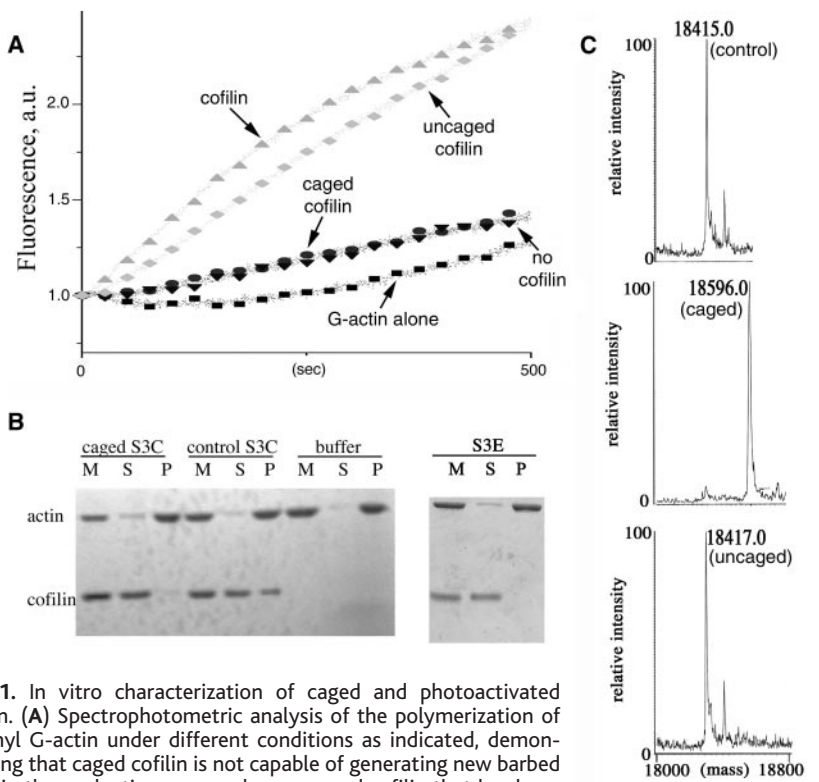

Fig. 1. In vitro characterization of caged and photoactivated cofilin. (**A**) Spectrophotometric analysis of the polymerization of pyrenyl G-actin under different conditions as indicated, demonstrating that caged cofilin is not capable of generating new barbed ends in the nucleation assay, whereas caged cofilin that has been activated by uncaging generates barbed ends comparable to unmodified S3C cofilin that has never been caged. All plots except that for G-actin alone have 300-nM F-actin seeds. (**B**) Coomassie blue–stained SDS–polyacrylamide gel electrophoresis (SDS-PAGE) of samples from a sedimentation assay of cofilin binding to F-actin. Mixtures (M) of 5 μM F-actin, equimolar S3C cofilin, S3E, or caged cofilin were incubated for 2 hours at room temperature and centrifuged for 20 min. SDS-PAGE analysis was performed on the pellet (P) and the supernatant (S) of each sample. Unmodified cofilin bound and pelleted with F-actin, whereas caged cofilin and S3E cofilin did not and remained in the supernatant. (**C**) Mass spectrometry data indicate the mass of control unmodified S3C (top), caged S3C (middle), and uncaged S3C (bottom). The presence of a single peak 181 mass units higher than the control indicates a complete conversion of S3C to caged S3C and then back to uncaged S3C on irradiation with 340-nm light. a.u., arbitrary units.

[1]Department of Anatomy and Structural Biology, [2]Department of Biochemistry, Albert Einstein College of Medicine, 1300 Morris Park Avenue, Bronx, NY 10461, USA.

*To whom correspondence should be addressed. E-mail: condeeli@aecom.yu.edu

described elsewhere (*18*). Using a nucleation assay to monitor severing and a sedimentation assay to monitor binding, we found that caged cofilin, like the constitutively inactive mutant S3E, did not bind to or sever F-actin (Fig. 1, A and B). Binding and severing were fully recovered after photoirradiation; thus, the caged cofilin mechanistically mimics inactive phosphocofilin. Furthermore, because the S3C form of cofilin cannot be phosphorylated by LIM-kinase (*18*), photouncaging generates a cofilin that is impervious to down-regulation by endogenous biochemical mechanisms. Mass spectrometric data (Fig. 1C) indicate that the protein was caged at a single site, and the failure to covalently modify the S3A mutant implicates Cys^3 as the chemically altered residue.

Single-site control of cofilin activity offers several advantages. First, it reduces the possibility of unintended nonspecific interactions between the caged inactive protein and other cytoplasmic proteins. Second, photoactivation of a singly caged protein can be achieved with a relatively efficient quantum yield, thereby reducing the amount of energy to which the cell is exposed. Finally, a single activation site markedly reduces the likelihood of generating an array of partially activated protein products. These properties suggest that the photoactivated form of caged cofilin is an ideal construct for assessing the intracellular consequences of cofilin action.

We first investigated the effects of global photorelease of S3C cofilin on F-actin content, the formation of free barbed ends, and the speed of cell locomotion. Caged cofilin (2 to 20 μM) was introduced into each carcinoma cell through microinjection (200 μM inside the needle). Cells containing caged cofilin were subsequently irradiated for 0.5 s, fixed either 10 min or 30 min after irradiation, and stained with fluorescent phalloidin, which binds to F-actin. We quantified the intensity of staining of Alexa-phalloidin in the injected cells by integrating the intensity of the labeled phalloidin in the entire cell body and subsequently normalizing it to the intensity of the labeled phalloidin in uninjected cells present in the same field. This value was plotted as a relative F-actin increase (Fig. 2C). Cells injected with caged cofilin and not irradiated did not display a significant increase in F-actin staining compared to neighboring cells in the same microscope field (Fig. 2, A and C). By contrast, a marked increase in F-actin content (36 ± 8%) was observed in irradiated cells containing caged cofilin (Fig. 2, B and C). The F-actin increase in these cells was highest at 10 min after irradiation and did not significantly decrease by 30 min. However, there was a higher cell-to-cell variability of F-actin content at 30 min. Active LIM-kinase inactivates cofilin by phosphorylation on Ser^3 in these carcinoma cells (*8*). The observation that photoreleased S3C remained active inside cells is consistent with the fact that the S3C mutant cannot be phosphorylated by LIM-kinase, as previously demonstrated in vitro (*18*). Our results indicate that there were no changes in F-actin content induced by irradiation or microinjection of the cells and that the F-actin increase was specific to the photorelease of S3C.

In order to assess the consequences of constitutive cofilin activity on F-actin content and to confirm the photoirradiation results, we injected both constitutively active S3A mutant and inactive S3E into cells and compared their F-actin content to uninjected cells. Final intracellular concentrations of the S3A and S3E mutants after microinjection were between 1.5 and 15 μM, whereas the endogenous cofilin level is 6 μM in these cells (*19*). Cells that had been injected with S3A displayed a 41 ± 19% increase in the amount of F-actin compared to uninjected cells (Fig. 2, E and F). Similarly, F-actin amounts were significantly elevated in cells injected with S3C (*20*). By contrast, cells microinjected with the inactive S3E mutant did not display significant increase in F-actin amounts (Fig. 2, D and F) (4 ± 5%). Cells injected with buffer only showed similar results. The increase in F-actin levels was independent of stimulation with epidermal growth factor (EGF), indicating that the activities of the mutant cofilins S3A and S3C inside the cell were unregulated by endogenous biochemical mechanisms. Furthermore, the F-actin increase was uniformly distributed throughout the entire cell body but not in stress fibers.

An increase in total intracellular level of F-actin should correspond to an increase in the free barbed end content. Therefore, we measured the effect of light-initiated cofilin activity on the generation of free barbed ends at the leading edge of cells. Cells were transfected with small interfering RNA (siRNA) against cofilin mRNA to decrease the expression of endogenous cofilin. Analysis of cell lysates by Western blotting showed an average of at least 90% reduction in cofilin levels. Cells treated with siRNA did not contain free barbed ends after stimulation with EGF (Fig. 2G). Barbed end production was rescued by microinjection of either active S3C or by photoactivation of caged S3C (Fig. 2, H and

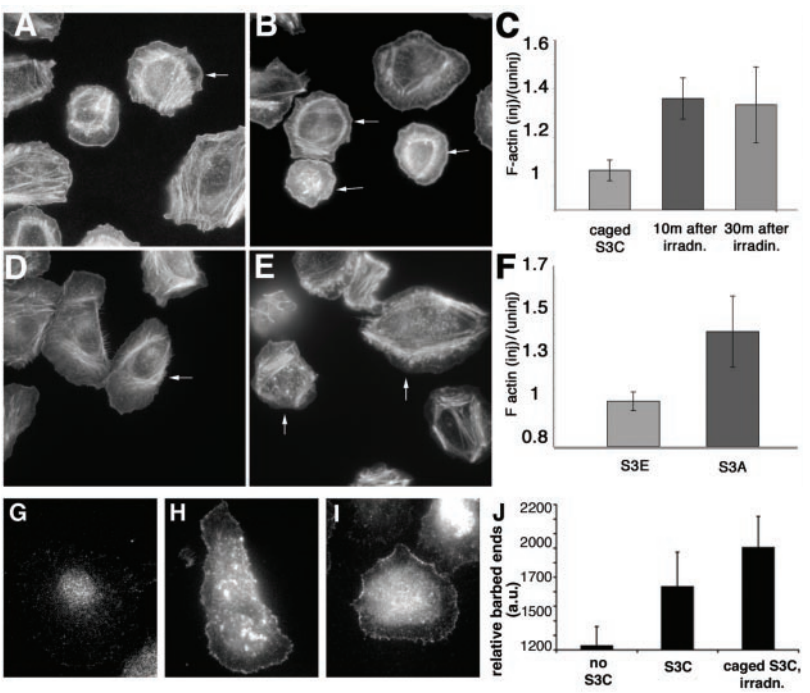

Fig. 2. (A to F) Global photoactivation of caged S3C in cells results in increased F-actin content. (**A**) MTLn3 cells were injected with caged S3C, which was not uncaged; arrows indicate injected cells. (**B**) Cells were injected with caged S3C and subsequently irradiated for 0.5 s to uncage S3C. (**C**) Measurement and quantification of the F-actin increase in the injected cells. Fluorescent intensities of F-actin stained with phalloidin of injected cells (inj) were normalized against neighboring uninjected cells (uninj). (**D**) Cells injected with S3E. (**E**) Cells injected with S3A. (**F**) Measurement and quantification of the F-actin increase in injected cells normalized against neighboring uninjected cells. All cells were fixed and immunostained with Alexa 684-phalloidin for quantification of F-actin. In each case, at least 20 cells were scored. (G to J) Global photorelease of cofilin leads to an increase in free barbed ends. (**G**) Treatment with siRNA against cofilin abolished free barbed ends in vivo. (**H** and **I**) barbed ends were rescued either (H) by microinjection of constitutively active S3C or (I) by injecting caged S3C followed by photoactivation. (**J**) Quantification of free barbed ends at the cell cortex for cells treated with siRNA and rescued by injection of S3C cofilin or by photorelease of caged cofilin (irradn) (*28*).

I, respectively). Thus, cofilin activity is necessary for the in vivo production of free barbed ends. Quantification of barbed end loss and subsequent rescue is presented in Fig. 2J. Identical suppression of barbed ends was obtained when constitutively active LIM-kinase was overexpressed in these cells to inactivate the endogenous cofilin by phosphorylation (*8*). Subsequent rescue of barbed ends was achieved through irradiation of cells that contained caged cofilin (*20*). Taken together, these experiments indicate that active cofilin increases F-actin content and generates free barbed ends in vivo. These experiments also demonstrate that photoirradiation of caged S3C can be used to generate free, active cofilin inside cells.

In the next set of experiments, MTLn3 cells were microinjected with caged S3C cofilin and illuminated in order to assess the effect of global photorelease on cell motility. Cell speed and behavior were recorded by time-lapse video microscopy before and after uncaging. The cells were traced in NIH Image software (*21*), and their average speed (velocity of cell locomotion), instantaneous speed (velocity of lamellipod protrusion), directionality (net path/total path length), persistence (speed/direction change), positive and negative flow (amount of new area formed/area lost in a given amount of time), and centroid position (mathematical center of mass) over time were computed with Dynamic Image Analsis Software (DIAS) (*22*). Cells injected with caged cofilin displayed an increase in instantaneous speed when irradiated, whereas uninjected cells did not (28% compared to cells not injected with caged cofilin, $P = 0.05$; 2-tailed, paired Student t test). The other DIAS parameters were not statistically different compared to cells that did not receive caged cofilin (*20*). Instantaneous speed is a measure of lamellipod size and velocity in cells that protrude and change shape more rapidly than they locomote (*23*, *24*). These results are consistent with the increased F-actin content in cells microinjected with caged cofilin followed by uncaging and demonstrates an increase in protrusive activity on cofilin photorelease that contributes to faster cell locomotion.

We next investigated the localized photorelease of cofilin in order to assess the effect of cofilin activity on protrusive activity and direction of cell locomotion. Caged cofilin was microinjected into MTLn3 cells, which are constitutively motile in media that contain serum. Cells were then locally irradiated in the cell cortex in a 3-μm-diameter spot for 2 s and time-lapse imaged to assess the effect of the local photorelease of cofilin activity over the next several minutes. Localized illumination induced the formation of a protrusion at the site of irradiation within 1 min after light exposure (Fig. 3, A to D). The cells were also exposed to a longer irradiation protocol in order to assess their total protrusion over 3 min. About 80% of all cells injected with caged cofilin displayed localized protrusions at the uncaging spot. Cells injected with caged cofilin and irradiated for 2 s showed a protrusion (+3% of total cell area) near the uncaging spot (Fig. 3I, $n = 6$ cells). The spot of illumination is coincident with the subsequently formed protrusion (Fig. 3, D and H, and Fig. 4D). In some cases, the protrusion emanated symmetrically from the site of illumination, and in other instances, protrusive activity was more asymmetric. On average, the geometrical center of the arc of protrusion (Fig. 3H, ϕ) lies within 16 ± 3° from the line drawn normal from the center of the uncaging spot to the cell surface. A longer uncaging protocol (exposure to 10 s of irradiation followed by 5 s of nonirradiation repeated over a total of 3 min) induced the formation of a larger protrusion (6%, $n = 14$ cells). Uninjected cells exposed to short pulses of light (2 s) failed to display any significant behavioral change ($n = 10$ cells). Instead, the longer irradiation protocol in uninjected cells led to a significant retraction from the site of illumination (Fig. 3I, $n = 7$ cells). Cells displayed spontaneous protrusions of 1 to 4% of the total cell area when locomoting in serum. Therefore, the protrusions produced by local uncaging of caged S3C can account for the majority of the protrusive activity of cells locomoting in serum.

To demonstrate that the protrusions were due to local uncaging of caged cofilin, we repeated the experiment in cells that lacked active endogenous cofilin by overexpressing constitutively active LIM-kinase. LIM-kinase inactivates endogenous cofilin through phosphorylation at Ser[3], and this suppresses the protrusion of lamellipodia (*8*). Local photoactivation of caged S3C cofilin induced protrusive activity in the region of illumination within 2 min, and by 10 min these sites displayed large lamellipods (Fig. 3, E to H).

Finally, cells were injected with caged cofilin, locally photouncaged, and allowed to locomote in serum in order to determine if localized activation of cofilin was sufficient to establish the direction of migration. Normally, under these conditions, MTLn3 cells exhibit random walking that is detected as a directionless diffusion-like movement of the cell centroid in perimeter plots (*25*). Caged cofilin was photoreleased with a sequential protocol of 10 s of illumination followed by 5 s in the dark over 3 min in a 3-μm spot. Spot illumination induced movement of the cell's centroid toward the uncaging spot during the period of uncaging and immediately thereafter (Fig. 4A, time lapse sequences). This was observed in ~70% of the irradiated cells ($n = 15$ cells) and is illustrated as perimeter plots that summarize all frames from the time lapse taken during and immediately after uncaging for three such cells in Fig. 4D. By

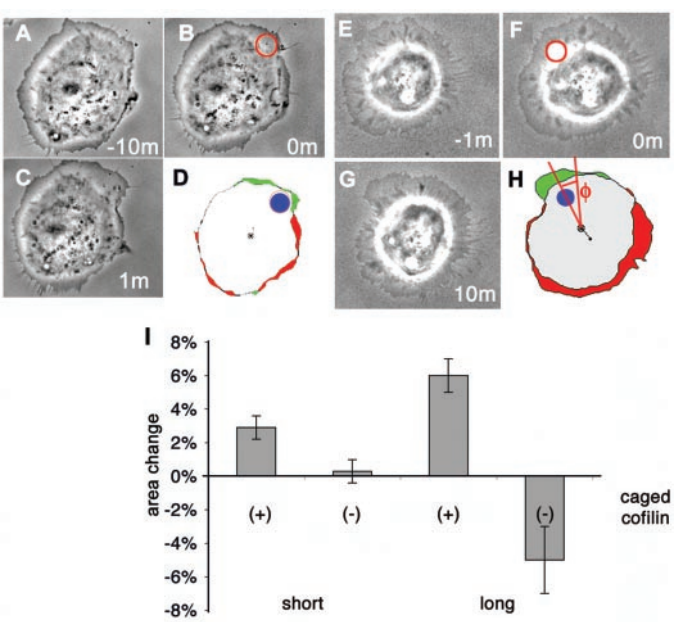

Fig. 3. (**A** to **D**) Local photorelease of caged cofilin causes local protrusion. (A) Constitutively motile MTLn3 cells in serum shown after injection of caged cofilin. (B) Cell before the start of irradiation, indicating the site of irradiation (orange circle). (C) 1 min after 2 s photoactivation. (D) DIAS perimeter plots of time-lapse images taken before and after photoactivation; showing the site of photoactivation (blue), protrusion (green), and retraction (red). (**E** to **G**) A time-lapse image of a MTLn3 cell expressing the kinase domain of LIM-kinase and microinjected with caged cofilin shows protrusion at the irradiated site. The protrusion was observed by 2 min and develops into a well-defined lamellipod by 10 min. All cells injected with caged cofilin showed the behavior indicated ($n = 4$ cells). (**H**) DIAS perimeter plot of the cell showing the area of protrusion in green and retraction in red, and the angle ϕ measuring the center of protrusion. (**I**) DIAS quantitation of the protrusion area due to uncaging as a percentage of the whole cell area. Cells with caged cofilin irradiated for 2 s (+) showed a protrusion (+4%) around the uncaging spot ($n = 6$ cells); the longer uncaging protocol caused larger protrusions (6%, $n = 14$ cells). Two-s irradiation of cells not injected with cofilin (–) did not generate any significant change in area ($n = 10$ cells), whereas the longer irradiation protocol led to a retraction of cell area ($n = 7$ cells).

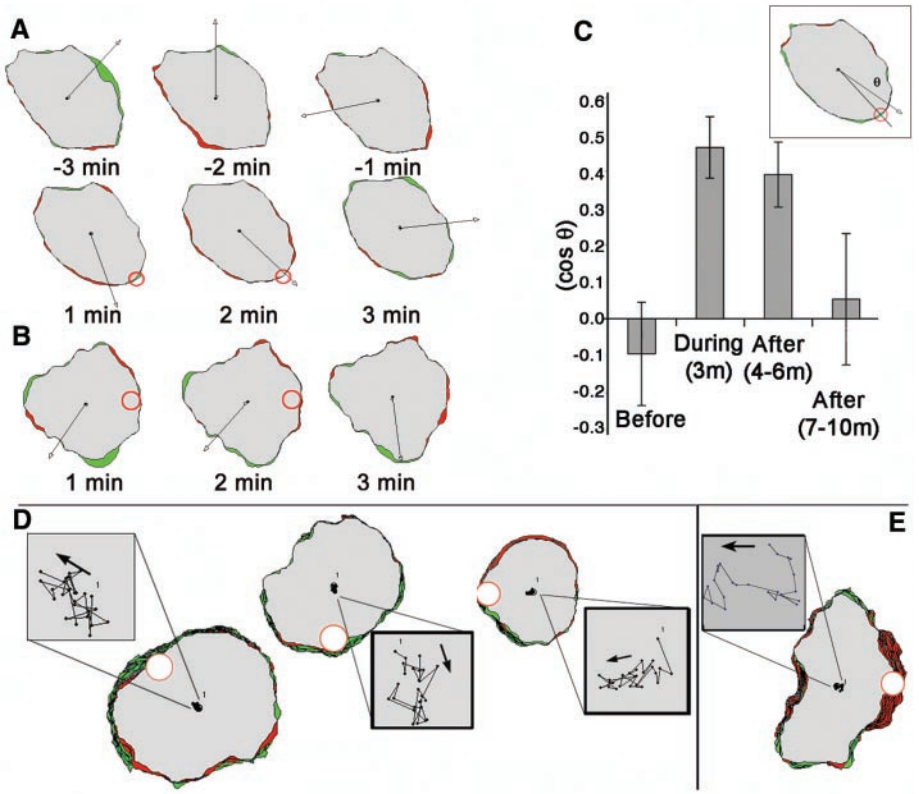

Fig. 4. Local photorelease of caged cofilin determines the direction of cell migration. Cells containing caged cofilin were locally irradiated over 3 min with the long irradiation protocol. (**A**) The direction of cell centroid movement at the time points indicated by "shape analysis" in DIAS, shown as an arrow emanating from the centroid. The red circle in frames 4 and 5 indicates the irradiation site. (**B**) Control cell. (**C**) The average of the cosine of the angle between the vector of centroid movement at the given time points and the uncaging spot. A positive cosine value indicates that the direction of locomotion is toward the cofilin uncaging site. Inset; The angle bounded by the arrow and the line joining the centroid to the uncaging spot θ was measured and its cosine value tabulated. (**D**) Perimeter and centroid movement (insets) plots of three typical cells microinjected with caged cofilin and irradiated at the site indicated. All migrated toward the irradiation site, building a protrusion that we can see by stacking time-lapse frames. (**E**) Perimeter and centroid plots of a typical control cell not microinjected with caged cofilin but irradiated. Control cells failed to protrude and usually retracted away from the site of uncaging (red). The arrow indicating the net direction of movement of the centroid was redrawn above the plots for clarity.

contrast, all control cells, which did not contain caged cofilin but were otherwise spot-irradiated in an identical fashion, showed no instantaneous response when illuminated (Fig. 4B) and eventually moved away from the uncaging spot (Fig. 4E, n = 9 cells). We quantified the directional response on cofilin photorelease by measuring the cosine of the angle between the position of the uncaging spot and the vector direction of the cell movement (Fig. 4C, inset) at times immediately before irradiation, 1 to 3 min during the course of irradiation, 1 to 3 min after the stop of irradiation, and 4 to 7 min after the stop of irradiation. The value of the cosine before irradiation was close to zero. During and immediately after irradiation, the vector plots rotated toward the uncaging spot, resulting in smaller angles and consequently positive cosine values. The effect disappeared by 4 to 7 min after the end of irradiation, as the direction of locomotion became random once more. The rate of disappearance of the effect was consistent with the duration of the motility cycle of 3 to 5 min after EGF stimulation (*19*, *26*) in cells with active LIM-kinase. Thus, the continuous localized production of active cofilin generates cell surface protrusions as well as sets the direction of cell motility.

In summary, we have employed a chemically engineered photoactivatable analog of cofilin to show that intracellular cofilin activity generates free barbed ends, polymerizes actin, induces protrusion, and sets the direction of cell migration. These observations are inconsistent with previous suggestions that the phosphorylation and inactivation of cofilin are necessary for motility to occur (*27*, *28*). Indeed, in contrast with motility models where cofilin is predicted to only depolymerize F-actin, our studies indicate that cofilin serves as a dynamic component of the steering wheel of the cell.

References and Notes

1. N. Yang *et al*., *Nature* **393**, 809 (1998).
2. H. Aizawa *et al*., *Nature Neurosci.* **4**, 367 (2001).
3. H. Aizawa, K. Sutoh, I. Yahara, *J. Cell Biol.* **132**, 335 (1996).
4. H. Abe, R. Nagaoka, T. Obinata, *Exp. Cell Res.* **206**, 1 (1993).
5. R. Nagaoka, H. Abe, K. Kusano, T. Obinata, *Cell Motil. Cytoskeleton* **30**, 1 (1995).
6. S. Ono, H. Abe, R. Nagaoka, T. Obinata, *J. Muscle Res. Cell Motil.* **14**, 195 (1993).
7. P. J. Meberg, J. R. Bamburg, *J. Neurosci.* **20**, 2459 (2000).
8. N. Zebda *et al*., *J. Cell Biol.* **151**, 1119 (2000).
9. K. S. McKim, C. Matheson, M. A. Marra, M. F. Wakarchuk, D. L. Baillie, *Mol. Gen. Genet.* **242**, 346 (1994).
10. Y. Samstag, E. M. Dreizler, A. Ambach, G. Sczakiel, S. C. Meuer, *J. Immunol.* **156**, 4167 (1996).
11. P. Roy *et al*., *J. Cell Biol.* **153**, 1035 (2001).
12. M. F. Carlier *et al*., *J. Cell Biol.* **136**, 1307 (1997).
13. J. R. Bamburg, *Annu. Rev. Cell Dev. Biol.* **15**, 185 (1999).
14. J. Condeelis, *Trends Cell Biol.* **11**, 288 (2001).
15. H. R. Dawe, L. S. Minamide, J. R. Bamburg, L. P. Cramer, *Curr. Biol.* **13**, 252 (2003).
16. J. Condeelis *et al*., in *Cell Motility: From Molecules to Organisms*, A. Ridley, M. Peckham, P. Clark, Eds. (Wiley, London, 2003), pp. 175–186.
17. I. Ichetovkin, W. Grant, J. Condeelis, *Curr. Biol.* **12**, 79 (2002).
18. M. Ghosh, I. Ichetovkin, X. Song, J. S. Condeelis, D. S. Lawrence, *J. Am. Chem. Soc.* **124**, 2440 (2002).
19. A. Y. Chan, M. Bailly, N. Zebda, J. E. Segall, J. S. Condeelis, *J. Cell Biol.* **148**, 531 (2000).
20. M. Ghosh *et al*., unpublished data.
21. NIH Image, National Institutes of Health, available at http://rsb.info.nih.gov/nih–image/.
22. D. R. Soll, *Int. Rev. Cytol.* **163**, 43 (1995).
23. D. Cox *et al*., *J. Cell Biol.* **116**, 943 (1992).
24. D. Cox, D. Wessels, D. R. Soll, J. Hartwig, J. Condeelis, *Mol. Biol. Cell* **7**, 803 (1996).
25. E. A. Shestakova, J. Wyckoff, J. Jones, R. H. Singer, J. Condeelis, *Cancer Res.* **59**, 1202 (1999).
26. M. Bailly *et al*., *J. Cell Biol.* **145**, 331 (1999).
27. M. Nishita, H. Aizawa, K. Mizuno, *Mol. Cell. Biol.* **22**, 774 (2002).
28. S. Arber *et al*., *Nature* **393**, 805 (1998).
29. Materials and methods are available as supporting material on *Science* Online.

30. Supported by research grant nos. GM61034 and GM38511 from the National Institutes of Health.

Supporting Online Material

www.sciencemag.org/cgi/content/full/304/5671/743/DC1

Materials and Methods

References and Notes

10 December 2003; accepted 31 March 2004